

*promoting access to White Rose research papers*



**Universities of Leeds, Sheffield and York**  
**<http://eprints.whiterose.ac.uk/>**

---

This is an author produced version of a paper published in **Organic Electronics**.

White Rose Research Online URL for this paper:

<http://eprints.whiterose.ac.uk/9783>

---

**Published paper**

Kingsley, J.W., Pearson, A.J., Harris, L., Weston S.J., Lidzey, D.G. (2009)  
*Detecting 6 MV X-rays using an organic photovoltaic device*, Organic Electronics, 10 (6), pp. 1170-1173

<http://dx.doi.org/10.1016/j.orgel.2009.06.006>

---

## Detecting 6 MV X-rays using an organic photovoltaic device

James W. Kingsley<sup>1</sup>, Andrew J. Pearson<sup>1</sup>, Lee Harris<sup>2</sup>,

Steven J. Weston<sup>2</sup> and David G. Lidzey<sup>1\*</sup>

<sup>1</sup>Department of Physics and Astronomy, The University of Sheffield,  
Hicks Building, Hounsfield Road, Sheffield S3 7RH, United Kingdom

<sup>2</sup>Medical Physics & Engineering, St. James's University Hospital,  
Leeds Teaching Hospitals Trust, Leeds LS9 7TF, United Kingdom

\* Author for correspondence: [d.g.lidzey@sheffield.ac.uk](mailto:d.g.lidzey@sheffield.ac.uk)

### Abstract

An organic photovoltaic (OPV) device has been used in conjunction with a flexible inorganic phosphor to produce a radiation tolerant, efficient and linear detector for 6 MV X-Rays. The OPVs were based on a blend of poly(3-hexylthiophene-2,5-diyl) (P3HT) and phenyl-C61-butyric acid methyl ester (PCBM). We show that the devices have a sensitivity an order of magnitude higher than a commercial silicon detector used as a reference. Exposure to 360 Grays of radiation resulted in a small (2%) degradation in performance demonstrating that these detectors have the potential to be used as flexible, real-time, in-vivo dosimeters for oncology treatments.

**Key Words:** Organic Photovoltaic, X-Ray, P3HT, PCBM.

## **Introduction**

X-ray imaging is used extensively in industry [1], medicine [2] and security [3]. In most medical and dental imaging systems, X-rays of energy between 50 and 100 kV are used, owing to the higher attenuation coefficient of bone compared to soft-tissue [2]. X-rays of significantly higher energy (up to 25 MV) are however used in the treatment of cancer [4,5]. Here, X-rays are directed to a localized region within the body (usually the site of a malignant tumour). The X-rays carry sufficient energy to generate ionisation in a region that is ideally localized within the tumour. This ionisation is in many cases sufficient to destroy the malignant tissue. There is a growing need [6] to routinely monitor the radiation dose provided to each individual patient during such radiation treatments with greater accuracy, and in particular provide a detailed real-time measure of the passage of radiation throughout the patient's body. This in-vivo dosimetry (IVD) is usually achieved by measuring the dose received by the patient using a MOSFET [7,8] or p-n junction diode placed on the surface of the patient's skin during each radiotherapy treatment [9]. Whilst this is difficult for single radiotherapy beams used in 3D conformal therapy, it is impossible to do for the highly modulated beams that are required for an intensity modulated radiotherapy treatment (IMRT) [10]. To perform in-vivo dosimetry for an IMRT treatment would require a large, conformal, spatially sensitive detector that can be placed in contact with the patient's body. Such a detector should necessarily be relatively transparent to the X-rays being used in the therapy.

To create such a detector clearly requires the use of an inherently flexible electronic device that can be fabricated over a large area and that is sensitive to the passage of X-rays. This combination of properties can be achieved by using an inorganic phosphor that is placed in contact with an organic photovoltaic device (OPV), with the OPV detecting luminescence emitted by the phosphor following the passage of the X-rays. Here, the use of an OPV is particularly beneficial as such devices can in principle be fabricated over relatively large areas onto a fully-flexible plastic substrate [11]. Indeed, an organic-semiconductor based system has recently been used to detect 70 kV X-rays used in medical imaging applications, with the device having sufficient level of radiation stability [12] and low dark-current [13] to make it suitable for

practical imaging applications. Other recent reports on the sensitivity of organic materials such as polyfluorenes and poly(triarylaminies) [14] and pentacene [15] to X-rays having an energy of 10's of kV also suggest such materials are often characterised by very promising levels radiation hardness, suggesting applications as electronic materials suitable for use in space-environments [15].

In this work, we focus on the detection of X-rays having higher energy (6 MV) using an OPV-based detector. Such X-rays are more highly penetrating (less well stopped) than those used in imaging (e.g. the total mass attenuation coefficient of 70 kV X-rays in SiO<sub>2</sub> is around 10 times greater than that of 6 MV X-rays [16]). Furthermore, the MV X-rays used in radiotherapy are typically delivered at dose-rates that are much larger than that used in imaging applications of ( $\sim$ 100 mGy s<sup>-1</sup> compared to < 1 mGy s<sup>-1</sup> [17]). A practical detector for such MV X-rays detector must therefore have a linear response over a wide exposure range, and be able to withstand the passage of a significant radiation flux through its active layer without its functionality being compromised by radiation-induced damage. Concerns arise however as to the ability of organic semiconductors to withstand the passage of a significant dose of MV X-rays without the generation of charge traps resulting from the local ionisation. Whilst kV X-rays have been shown to generate a sufficient quantity of luminescence within a thin scintillator film that is detectable by an OPV [12, 13], it is not clear whether significantly more penetrating X-rays of interest here would generate a detectable optical signal. As we report however, the devices that we have created have a sensitivity that is an order of magnitude better than that of a conventional (small-area) silicon p-n junction based device. Furthermore, we show that the organic X-ray detector prototyped is remarkably radiation tolerant, with only a small loss (2%) in sensitivity measured over the course of a relatively large (360 Gy) radiation exposure.

## Experimental

The OPVs that we have used are based on a thin film blend of the conjugated polymer poly(3-hexylthiophene) [P3HT] and the fullerene derivative PCBM. This material system currently represents the

state of the art for organic photovoltaic devices, with the highest external quantum efficiencies (EQE) recorded being around 80% at 500 nm [18, 19]. A schematic of the devices fabricated is shown in figure 1. Briefly, devices are fabricated by spin-casting a layer of PEDOT:PSS onto an ITO anode which is then baked in N<sub>2</sub> for 10 minutes at 100 °C to remove adsorbed water. The substrates are then transferred to an overpressure nitrogen glovebox, where an 1:0.8 (by mass) blend solution of P3HT:PCBM in chlorobenzene is spin-cast onto the ITO/PEDOT:PSS anode. A cathode consisting 100 nm of aluminium is then evaporated onto the organic thin film at a base pressure of <10<sup>-6</sup> mBar. The devices are encapsulated by bonding a 0.5 mm glass sheet onto their surface using a UV curable glue. Finally, the devices are annealed at 150 °C for 60 minutes. Measurements using a calibrated solar-simulator operating at 100 mW cm<sup>-2</sup> (Oriel Instruments AM1.5 solar simulator calibrated with an NREL 4 cm<sup>2</sup> silicon reference cell) indicate that the devices have a typical power conversion efficiency (PCE) of 3.7% immediately following fabrication. However, since OPVs undergo a period of degradation when initially illuminated, the devices were aged for 30 minutes under 1 sun (AM 1.5) illumination to improve their stability. This process resulted in devices with a typical PCE of 3%. The measured EQE of the OPV devices is shown in figure 1. Here, it can be seen that our devices have a peak EQE of 57% at 504 nm (post aging). Each device has an active area of 4.5 mm<sup>2</sup>, which is defined by the overlap of the anode and cathode strips.

As a phosphor we have used the material Gd<sub>2</sub>O<sub>2</sub>S:Tb. This was purchased from Applied Scintillation Technologies in the form of a flexible substrate that was coated with the phosphor at an area density of 279 mg/cm<sup>2</sup>. In the experiments described, the substrate was placed in direct contact with the OPV such that luminescence emitted was directly incident upon the transparent anode. To evaluate the efficiency of the composite detector, we have used the linear accelerator facility at St. James's University Hospital in Leeds. The machine forms part of a dedicated research facility, however the linac is typical of a machine used to deliver megavoltage radiotherapy treatments around the world. This machine provides 6 MV X-rays up to a maximum dose rate of ~100 mGy s<sup>-1</sup> (approximately equivalent to 10<sup>14</sup> photons s<sup>-1</sup> m<sup>-2</sup>).

## Results and Discussion

The MV X-rays studied here can interact with matter in one of two ways; by Compton scattering and via pair-production. In both processes, a high-energy electron (or positron) is forward scattered (by a distance of  $\sim 1.5$  cm in water), producing a shower of secondary ionisation. In radiation therapy these low-energy ( $< 100$  keV) secondary electrons are used to deliver the energy that destroys malignant tissue. In our detector, the secondary electrons created excite the  $\text{Gd}^{3+}$  (which is contained within a ceramic host-matrix) that then transfers its energy to the rare-earth  $\text{Tb}^{3+}$  dopant [20,21]. The luminescence from the  $\text{Tb}^{3+}$  is then detected by the OPV. The emission spectra of phosphor recorded under X-ray illumination is shown in figure 2. It can be seen that the peak emission wavelength (540 nm) coincides well with the peak sensitivity of the OPV (504 nm), ensuring efficient detection. Indeed, from the overlap integral of the two spectra, we calculate that in an idealised device (i.e. having no optical loss), the luminescent photons should be detected with an efficiency of 44%.

Figure 3(a) plots the photocurrent from the device as a function of X-ray dose rate. We find that the X-rays are detected with a sensitivity of  $0.086 \text{ C m}^{-2} \text{ Gy}^{-1}$  over the entire range of dose-rates explored, confirming the applicability of the device as a dosimeter. Control experiments in which no phosphor layer was used show that X-rays can be detected directly by the OPV itself but that the sensitivity is over two orders of magnitude lower. This relative insensitivity of the OPV to direct exposure to X-rays results from the fact that the active semiconductor is relatively thin ( $\sim 150$  nm in total), and thus the rate of charge generation within the OPV semiconductor layers is very low. We can also estimate the quantum efficiency ( $\eta$ ) of the device (photoelectrons per X-ray absorbed in the phosphor) using  $\eta = k/\gamma$  where  $k$  is the rate at which electrons are produced (calculated directly from the current) and  $\gamma$  is the rate at which X-rays are absorbed. The rate at which X-rays are absorbed is calculated using  $\gamma = \rho D A / E$  where  $\rho$  is the sheet density of the phosphor,  $D$  is the dose rate,  $A$  is the pixel area and  $E$  is the average energy of an X-ray (which is a third of the acceleration voltage). This leads to an overall efficiency of  $\sim 62,000$  electrons per absorbed X-ray photon. By dividing this figure by the OPV luminescent photon detection efficiency and assuming an

optical loss of a half, we estimate the phosphor yield to be 47,000 photons per MeV. This value compares favourably with similar scintillators in the literature [22].

For comparison, we have also recorded the current generated by a commercial (Scanditronix EDP-10) silicon p-n junction based X-ray detector under identical conditions to that described above. This device is based on a silicon detector that is encapsulated within a stainless-steel / epoxy block (6.5 mm thick x 12 mm diameter), and works by directly collecting the ionised charge produced within the detector (rather than via the detection of luminescence). Encouragingly, we find that the photocurrent produced by the OPV/phosphor detector was  $\sim$ 14 times larger than that recorded from the silicon-based devices when exposed to the same radiation flux. We note that a similar combination of OPV and an  $\text{Gd}_2\text{O}_2\text{S:Pr}$  phosphor have been used [12] to detect 70 kV X-rays. In such previous work, the lower energy X-rays were detected with a sensitivity of  $1.28 \text{ C m}^{-2} \text{ Gy}^{-1}$  (when the OPV was run in short-circuit mode); a factor of  $\sim$  15 times higher than that demonstrated here. We believe that the 10 times higher penetration depth of the 6 MV X-rays used here most likely accounts for this difference in sensitivity.

It is clear that our device works as a radiation detector, however it is important to assess its relative stability under continuous exposure to X-rays. Devices were therefore subjected to prolonged operation (with phosphor present) and the output current monitored. This is plotted in figure 3(b) in which it can be seen that over the course of the exposure - which lasts a period of 60 minutes and corresponds to a total radiation dose of 360 Gy - the detected photocurrent drops by around 2%. Measurements of the OPV PCE after such exposure failed to identify any significant degradation in device efficiency, demonstrating a relatively promising level of stability. Indeed, the typical dose received by a device during an individual radiation therapy treatment would be  $\sim$  2 Gy, indicating that our un-optimized detector could survive many individual radiation exposures. We believe the relative radiation stability of an OPV results from the fact that the organic semiconductor layer used in the OPV is very thin (conjugated polymers are direct-gap semiconductors and thus have very high extinction coefficients). For this application, this relative thinness is a distinct advantage as the rate of damage that occurs to the organic-semiconductor via direct interaction

with the highly penetrating (and thus weakly interacting) MV X-rays is low. This observation is commensurate with the fact that the directly-generated photocurrent within the OPV is also low.

Finally, transparency is an important feature of any thin-film device that is to be used in real-time dosimetry during radiation therapy. We have therefore used the commercial silicon detector described above to determine the attenuation in X-ray flux passing through either the OPV, or the phosphor, or the stacked OPV and phosphor. We find that the intensity X-ray beam is attenuated by a 1.3% when passing through the phosphor, by 1.7% when passing through the OPV and thus by 3% when passing through the entire stacked device. This is a relatively low rate of attenuation, and would not compromise the efficacy of a typical radiation treatment.

## Conclusions

We have prototyped a MV X-ray detector consisting of a flexible phosphor layer in contact with an organic photovoltaic fabricated from P3HT:PCBM. X-rays incident on the phosphor generate luminescence that is then detected by the organic photovoltaic. In order to increase stability of the detectors, the organic photovoltaics were aged for 30 minutes under AM 1.5 simulated sunlight in order to remove any initial degradation in performance, however, even after this process the external quantum efficiency was greater than 55% at the peak wavelength emitted by the phosphor. This well matched spectral response between the phosphor and the organic photovoltaic resulted in a device having a sensitivity higher than a commercial silicon detector. The system also had excellent radiation hardness with less than 2% variance in output recorded over 360 Grays of radiation dose. Our measurements therefore suggest that organic detectors may find application as real-time, patient-specific dosimeters used in the imaging of X-rays for radiotherapy treatment.

## Acknowledgements

We thank the UK EPSRC for funding this work via grants EP/F016433 (Optimising polymer photovoltaic devices through control of phase-separation) and EP/F056370 (High-efficiency block copolymer solar cells – a scaleable prototype for low cost energy generation). We also thank John McMillan (University of Sheffield) for useful and enlightening discussions.

## References

- [1] R.R. da Silva, D. Mery, *Insight*, 49 (2007) 603-609.
- [2] P. Suortti, W. Thomlinson, *Phys. Med. Biol.* 48 (2003) R1-R35.
- [3] A. Olivo, D. Chana, R. Speller, *J. Phys. D: Appl. Phys.* 41 (2008) 225503.
- [4] J.T. Parsons, B.D. Greene, T.W. Speer, S.A. Kirkpatrick, D.B. Barhorst, T. Yanckowitz *International Journal of Radiation Oncology Biology Physics* 50 (2001) 953-959.
- [5] D. Followill, P. Geis, A. Boyer, *International Journal of Radiation Oncology Biology Physics* 38 (1997) 667-672.
- [6] M.K. Bucci, A. Bevan, M. Roach *CA Cancer J. Clin.* 55 (2005) 117-134.
- [7] T. Kron, L. Duggan, T. Smith□, A. Rosenfeld, M. Butson, G. Kaplan, S. Howlett, K. Hyodo, *Phys. Med. Biol.* 43 (1998) 3235–3259.
- [8] M.J. Butson, T. Cheung, P.K.N. Yua, *Applied Radiation and Isotopes* 62 (2005) 631 – 634.
- [9] M. Essers & B.J. Mijnear *Int. J. Radiat. Oncol. Biol. Phys.* 43 (1999) 245-59.
- [10] E.B Podgorsak and M.B. Podgorsak *IAEA Radiation Oncology Physics: A Handbook for Teachers and Students* 534-536, Ed. E.B. Podgorsak, International Atomic Energy Agency, Vienna (2005).
- [11] S.-I. Na, S.-S. Kim, J. Jo, D.-Y. Kim, *Adv. Mater.* 20 (2008) 4061-4067.
- [12] R.E. Keivanidis, N.C. Greenham, H. Sirringhaus, R.H. Friend, J.C. Blakesley, R. Speller, M. Campoy-Quiles, T. Agostinelli, D.D.C. Bradley, J. Nelson, *Appl. Phys. Lett.* 92 (2008) 023304.

- [13] T. Agostinelli, M. Campoy-Quiles, J.C. Blakesley, R. Speller, D.D.C. Bradley, *Appl. Phys. Lett.* 93 (2008) 203305.
- [14] C.R. Newman, H. Sirringhaus, J.C. Blakesley, R. Speller, *Appl. Phys. Lett.* 91 (2007) 142105.
- [15] R.A.B. Devine, M-M Ling, A.B.Mallik, M. Roberts, Z. Bao, *Appl. Phys. Lett.* 88 (2006) 151907.
- [16] Engineering Compendium on Radiation Shielding, eds. R.G. Jaeger, E.P. Blizzard, A.B. Chilton, M. Grotenhuis, A. Höning, Th. A. Jaeger, H.M. Eisenlohr, pub. Springer-Verlag, Berlin/Heidelberg, 2 (1975) 183.
- [17] K.C. Young, M.L. Ramsdale, A. Rust, J. Cooke, *The British Journal of Radiology* 70 (1997) 1036-1042.
- [18] S.-H. Jin, B.V.K. Naidu, H.-S. Jeon, S.-M. Park, J.-S. Park, S.C. Kim, J.W. Lee, Y.-S. Gal *Solar Energy Materials & Solar Cells* 91 (2007) 1187–1193.
- [19] M. Lenes, G.-J.A.H. Wetzelaer, F.B. Kooistra, S.C. Veenstra, J.C. Hummelen, P.W.M. Blom, *Adv. Mater.* 20 (2008) 2116–2119.
- [20] S.W. Allison, M.R. Cates, G.T. Gillies *Rev. Sci. Inst.* 73 (2002) 1832-1834.
- [21] E.I. Gorokhova, V.A. Demidenko, S.B. Rodnyi, C.W.E. van Eijk, *IEEE Transactions on Nuclear Science* 52 (2005) 3129-3132.
- [22] P. Leecoq, A. Annenkov, A. Gekhtin, M. Korzhik, C. Pedrini, *Inorganic Scintillators for Detector Systems: Physical Principles and Crystal Engineering*, pp 25 (2006) Springer, New York.

## Figure captions

Figure 1. Schematic of the detector operation (color online). The incident X-rays (red) produce a forward-scattered primary electron (blue) which then produces secondary ionization electrons (yellow). This secondary ionization excites the phosphor, whose luminescence (green) is detected by the organic photovoltaic device.

Figure 2. The external quantum efficiency of the organic photovoltaic device shown together with X-ray excited luminescence spectra of the phosphor.

Figure 3. Part (a) shows a log-log plot of output current versus X-ray dose rate for the OPV both with and without the phosphor present as well as for the reference silicon detector. Part (b) shows the current recorded from the device as a function of time whilst exposed to a constant X-ray dose rate of  $\sim 100 \text{ mGy s}^{-1}$ .

Figure 1

[Click here to download high resolution image](#)

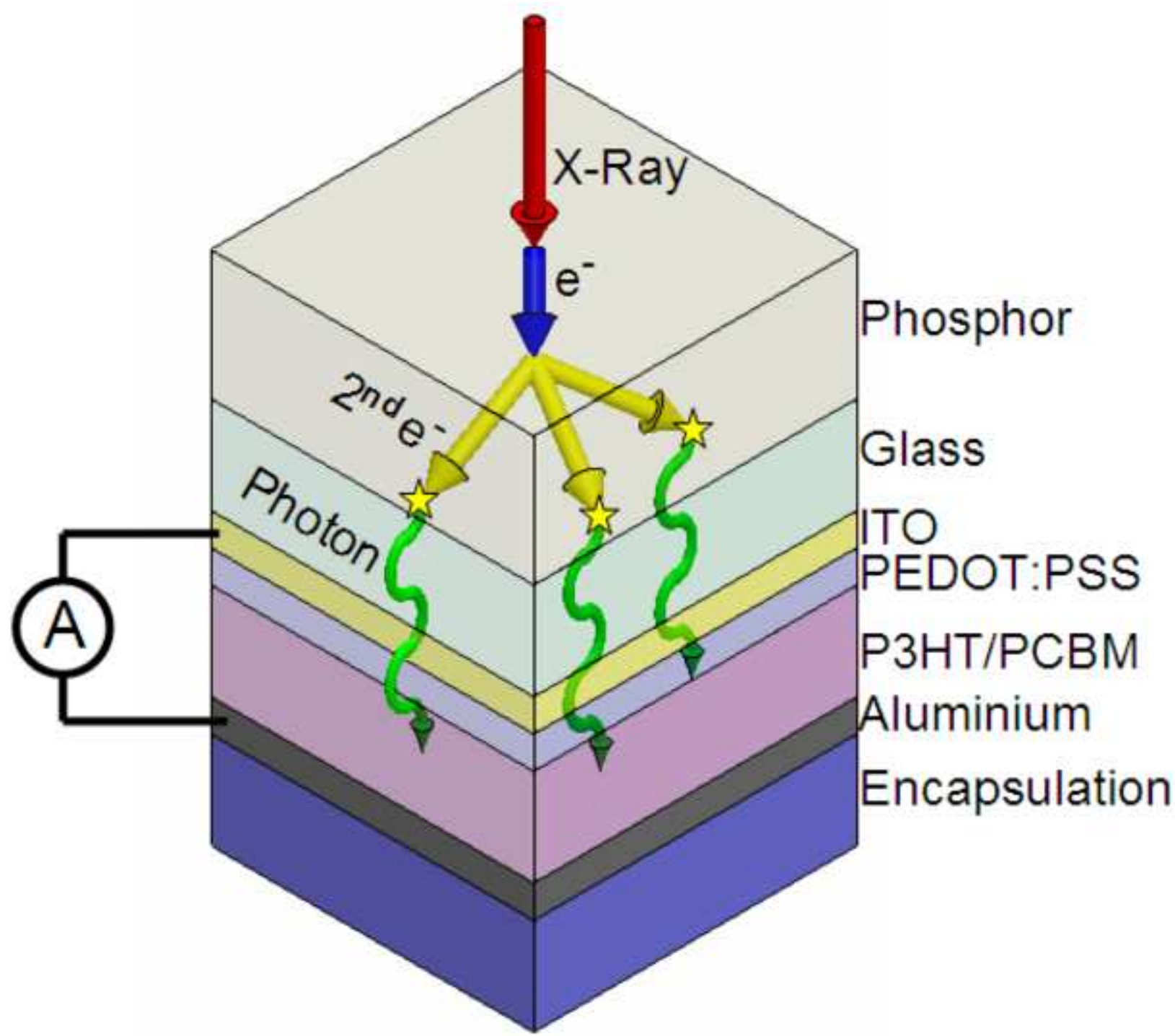


Figure 2

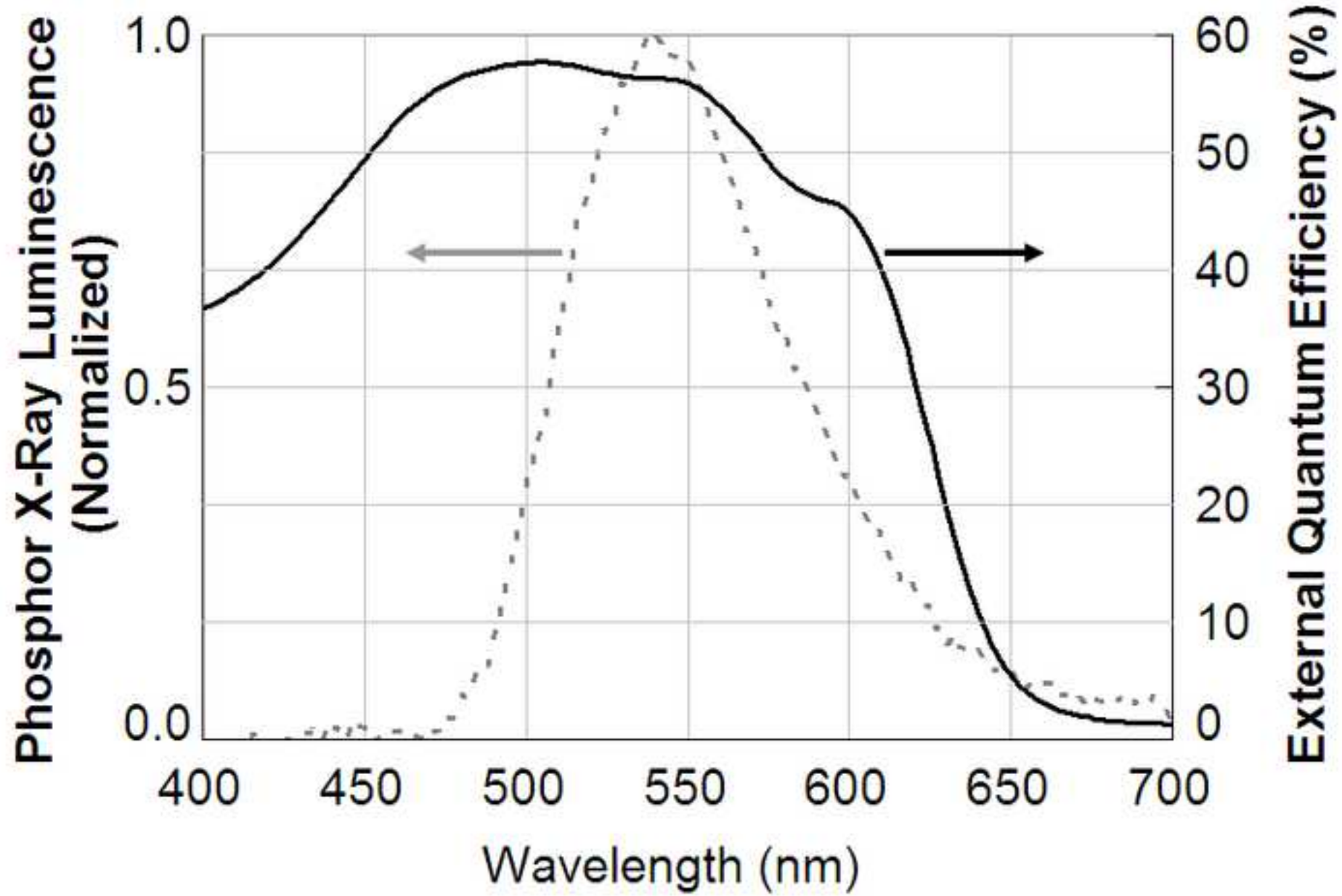
[Click here to download high resolution image](#)

Figure 3

[Click here to download high resolution image](#)